CRYSTAL GROWTH & DESIGN

Article

pubs.acs.org/crystal

Construction of Three-Dimensional Cobalt(II)-Based Metal–Organic Frameworks by Synergy between Rigid and Semirigid Ligands

Weiting Yang, Min Guo, Fei-Yan Yi, and Zhong-Ming Sun*

State Key Laboratory of Rare Earth Resource Utilization, Changchun Institute of Applied Chemistry, Chinese Academy of Sciences Changchun, 130022, China

Supporting Information

ABSTRACT: Solvothermal assembly of Co(II) ion, a semirigid tetrahedral carboxylate ligand tetrakis[(4-carboxyphenyl)oxamethyl]-methane acid (H_4L), and rigid linear bidentate linker 1,4-di(1*H*-imidazol-1-yl)benzene (dib) or 4,4′-di(1*H*-imidazol-1-yl)-1,1′-biphenyl (dibp) yields four novel metal–organic frameworks (**1**–**4**) with different topological connections. $[Co_2(L)(dib)]\cdot 3DMF$ (**1**) is a 2-fold interpenetrating *sqc*422 network and contains 3-dimensional interconnected channels along [100], [010], and [110] directions; $[Co_4(L)_2(dib)_3(H_2O)_4]\cdot 4H_2O$ (**2**) is a three-dimensional 3,4,4-connected new topology with 5-fold interpenetration; $[Co_2(L)(dibp)]\cdot 5DMF$ (**3**) and $Co_2(L)(dibp)_2$ (**4**) are formed in the presence of dibp linker; they feature three-dimensional novel topologies based on 4,6-connection and 4,4-connection, respectively, and no interpenetration is observed. It is demonstrated that interpenetration is accessible simply by changing auxiliary ligands and solvents. Magnetic studies reveal that complexes **1** and **3** exhibit antiferromagnetic behavior.

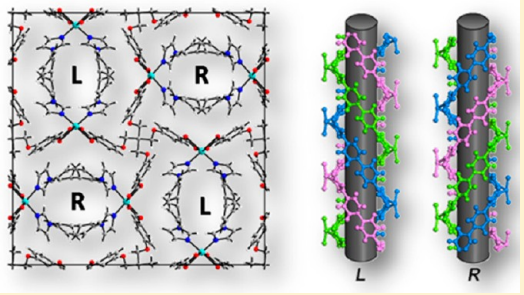

INTRODUCTION

Metal–organic frameworks (MOFs) represent a class of porous inorganic–organic solid state materials which are built from metal ions and organic linkers. Their well-defined porosity and tunable functionality make them extremely attractive for applications in gas adsorption and storage,[1] drug release,[2] sensing,[3] catalysis,[4] etc. As applications rely heavily on the structures, one hot research area is to synthesize various novel structures generally by judicious selection of organic linkers and inorganic molecular building blocks to construct tailored frameworks with desired properties.[5] As a semirigid tetrahedral ligand, tetrakis[(4-carboxyphenyl)oxamethyl]methane acid (H_4L) possesses four carboxylate arms, which can twist around the quaternary carbon center by different angles to adapt different coordination environments. Until now, a number of MOFs constructed from this ligand have been reported, including both interpenetrating and noninterpenetrating frameworks with rich structural diversities.[6]

Auxiliary ligands are widely used in the syntheses of new MOF architectures. A lot of MOF structures based on mixed organic ligands have been demonstrated.[7] Recently, the use of semirigid ligands combined with second linkers to construct novel MOFs has been studied. For example, Du and co-workers reported metal–organic coordination polymers, which are formed by tetrahedral quadridentate linker TPOM (TPOM = tetrakis(4-pyridyloxymethylene)methane) and bidentate D-H_2cam or benzene-1,4-dicarboxylic acid ligand.[8] The second ligands they used are acidic species. Since two different functional ligands have effects on the connection between the metal ions and the organic ligands in the structure, as well as on charge density distribution, we chose a basic second linker to help a C_3 symmetric semirigid ligand, 4-[3-(4-carboxyphenoxy)-2-[(4-carboxyphenoxy)methyl]-2-methylpropoxy]-benzoate, to build MOFs, and obtained two novel Zn-based MOFs.[9] As further expansion of these studies, herein we report the syntheses, structures, and magnetic properties of four novel MOFs (**1**–**4**) based on semirigid tetrahedral carboxylate ligand L in presence of secondary imidazole ligands, dib (1,4-di(1*H*-imidazol-1-yl)benzene) and dibp (4,4′-di(1*H*-imidazol-1-yl)-1,1′-biphenyl).

EXPERIMENTAL SECTION

Materials and Measurements. All reagents and solvents for syntheses were commercially available and used without further purification. H_4L was synthesized according to the documented procedures.[10] 1,4-di(1H-imidazol-1-yl)benzene (dib) and 4,4′-di(1H-imidazol-1-yl)-1,1′-biphenyl (dibp) were obtained from Jinan Henghua Sci. & Tec. Co., Ltd. X-ray powder diffraction (XRD) data were collected on a D8 Focus (Bruker) diffractometer at 40 kV and 30 mA with monochromated Cu Kα radiation (λ = 1.5405 Å) with a scan speed of 5 deg/min and a step size of 0.02° in 2θ. Inductively coupled plasma (ICP) analyses of Co and elemental analyses of C, H, and N were conducted on a Perkin-Elmer Optima 3300DV spectrometer and a Perkin-Elmer 2400 elemental analyzer, respectively. Thermogravimetric and differential thermal analysis (TG-DTA) data were recorded on a thermal analysis instrument (SDT 2960, TA Instruments, New Castle, DE) from room temperature to 800 °C with a heating rate of 10 °C/min under nitrogen atmosphere. Temperature-dependent

Received: August 1, 2012
Revised: September 11, 2012
Published: September 14, 2012

Table 1. Crystal Data and Structure Refinement Results for Complexes 1−4

	1	2	3	4
formula	$C_{45}H_{34}N_4O_{12}Co_2$	$C_{51}H_{45}N_6O_{16}Co_2$	$C_{102}H_{76}N_8O_{24}Co_4$	$C_{69}H_{52}N_8O_{12}Co_2$
fw	940.62	1115.73	2033.43	1303.04
T (K)	293(2)	293(2)	293(2)	293(2)
λ (Å)	0.71073	0.71073	0.71073	0.71073
space group	*Pccn* (No. 56)	$P\bar{1}$ (No. 2)	*C*2/*c* (No. 15)	$I\bar{4}2d$ (No. 122)
a (Å)	20.131(2)	9.0384(10)	20.930(4)	26.658(2)
b (Å)	24.767(3)	16.3407(18)	52.180(10)	26.658(2)
c (Å)	26.928(3)	18.505(2)	30.679(6)	8.4790(6)
α (deg)	90	73.394(2)	90	90
β (deg)	90	76.394(2)	104.625(2)	90
γ (deg)	90	86.298(2)	90	90
V (Å^3)	13426(3)	2545.6(5)	32419(5)	6025.7(8)
Z, ρ_{calcd} (g/cm^3)	8, 0.931	2, 1.445	8, 0.833	4, 1.436
μ(Mo Kα) (mm^{-1})	0.538	0.728	0.449	0.624
GOF on F^2	1.024	0.975	0.959	1.086
R_1 [$I > 2\sigma(I)$]^a	0.0988	0.0997	0.0495	0.0795
wR_2^{a}	0.2793	0.2857	0.0954	0.2306
Flack				0.03(4)

$^aR_1 = \sum||F_o| - |F_c||/\sum|F_o|$. $wR_2 = \{\sum w(F_o^2 - F_c^2)^2/\sum[w(F_o^2)^2]\}^{1/2}$.

magnetic susceptibility data were recorded on a Quantum-Design MPMS-XL SQUID magnetometer under an applied field of 1000 Oe over the temperature range of 2−300 K.

Syntheses. *Synthesis of [Co_2(L)(dib)]·3DMF (1).* Compound **1** could be readily synthesized by the solvothermal reaction. A suspension of $Co(NO_3)_2·6H_2O$ (0.24 mmol), H_4L (0.05 mmol), and dib (0.05 mmol) in 10 mL of DMF (*N*,*N*-dimethylformamide) was sealed in a 25 mL Teflon-lined stainless steel autoclave and heated under autogenous pressure at 130 °C for 72 h. After the autoclave was cooled to room temperature, purple block single crystals suitable for single-crystal X-ray crystallographic analysis were obtained. Then, the resulting crystals were rinsed three times with DMF and dried at room temperature overnight for further characterization. Yield: 85 mg (61% based on Co^{2+}).

Synthesis of [Co_4(L)$_2$(dib)$_3$(H_2O)$_4$]·4H_2O (2). The synthesis of compound **2** is similar to that of compound **1**, except for the solvent used. Compound **2** was obtained with a mixed solvent of 5 mL of DMF and 5 mL of deionized water; in addition, the $Co(NO_3)_2·6H_2O$ was reduced to 0.12 mmol. Purple block single crystals were produced. Yield: 82.5 mg (58% based on Co^{2+}).

Synthesis of [Co_2(L)(dibp)]·5DMF (3). The synthesis of compound **3** is similar to that of compound **1**, except that dibp was used instead of dib. Purple block single crystals were synthesized. Yield: 129.3 mg (76% based on Co^{2+}).

Synthesis of Co_2(L)(dibp)$_2$ (4). The synthesis of compound **4** is similar to that of compound **2**, except that dibp was used instead of dib. Purple block single crystals were obtained. Yield: 109.3 mg (70% based on Co^{2+}).

Crystallography. Single crystals with suitable dimensions for **1**−**4** were selected for single-crystal X-ray diffraction analyses. Data collections were performed on a Rigaku RAXIS-RAPID diffractometer equipped with graphite-monochromated Mo Kα radiation (λ = 0.71073 Å) at a temperature of 293 K. Data reductions and absorption corrections were performed using the SAINT and SADABS software packages, respectively.[11] The structure was solved by direct methods and refined on F^2 by full-matrix least-squares using SHELXTL97 crystallographic software package.[12] All of the non-hydrogen atoms were found from the difference Fourier map and refined anisotropically. The hydrogen atoms associated with the organic ligands were generated geometrically and included in the refinement with fixed position and thermal parameters. Although the TGA and elemental analysis results of **1** and **3** implied the existence of extraframework DMF, they could not be located in the difference Fourier maps derived from the poor single crystal data. Efforts to obtain better crystal data have failed. Further details of the structure analyses are listed in Table 1. The selected bond lengths and bond angles are listed in Table S1 in the Supporting Information. The powder X-ray diffractions of these compounds confirm the phase purities (see Supporting Information Figures S1−S4). Elemental analysis observed (calcd): Co 9.89% (10.16%), C 56.78% (55.88%), H 4.96% (4.74%), N 7.96% (8.45%) for **1**; Co 10.64% (10.58%), C 55.89% (54.95%), H 4.15% (3.86%), N 7.06% (7.54%) for **2**; Co 8.46% (8.53%), C 58.00% (57.32%), H 5.94% (5.28%), N 9.26% (9.12%) for **3**; Co 9.44% (9.04%), C 63.77% (63.54%), H 4.17% (3.99%), N 8.78% (8.59%) for **4**. The bond valence sum (BVS) calculation indicates that all the cobalt ions are normally divalent (BVS 2.244 (Co1) and 2.192 (Co2) for **1**, 1.964 (Co1) and 1.839 (Co2) for **2**, 2.15 (Co1), 2.125 (Co2), 2.091 (Co3), and 2.106 (Co4) for **3**, and 2.172 (Co1) for **4**.

RESULTS AND DISCUSSION

Structure of 1. The single-crystal diffraction analysis of compound **1** reveals a three-dimensional (3-D) coordination framework. The asymmetric unit of **1** consists of two crystallographically independent Co atoms, one L ligand, and one dib ligand. As depicted in Figure 1, both of the Co atoms are five coordinated by four oxygen atoms from four carboxylate groups in L ligand and one nitrogen atom of dib. These coordination environments make a distorted square pyramid geometry. The $Co(1)O_4N$ and $Co(2)O_4N$ square

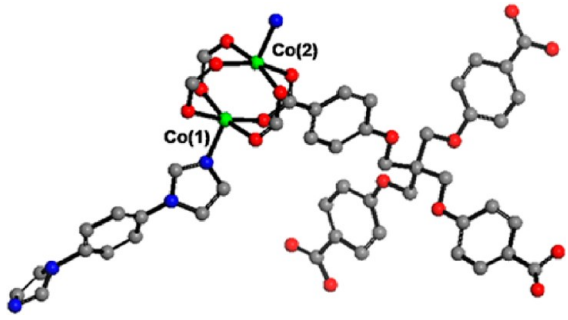

Figure 1. Coordination environments in **1** giving the dimetallic building unit (cobalt, green; carbon, gray; nitrogen, blue; oxygen, red). Hydrogen atoms are omitted for clarity.

dx.doi.org/10.1021/cg301094h | *Cryst. Growth Des.* 2012, 12, 5529−5534

pyramids are connected to each other via four carboxylate groups to form a dinuclear cluster. As seen in Figure 2, such

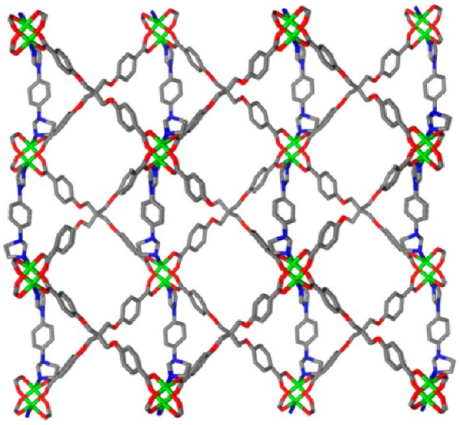

Figure 2. One independent single net in the interpenetrating framework of **1** (cobalt, green; carbon, gray; nitrogen, blue; oxygen, red). Hydrogen atoms are omitted for clarity.

dimetallic building units are linked together by L ligands resulting in a 3-D framework, in which the second linker dib is inserted between two dimetallic building units. The whole framework of **1** is 2-fold interpenetrated with 3-D interconnected channels ([100] 5.80 × 5.80 Å, [010] 4.97 × 4.66 Å, [110] 4.51 × 3.65 Å). All pore sizes in this work are calculated through taking into account the van der Waals radius (Figure 3). As estimated by the PLATON program,[13] the potential

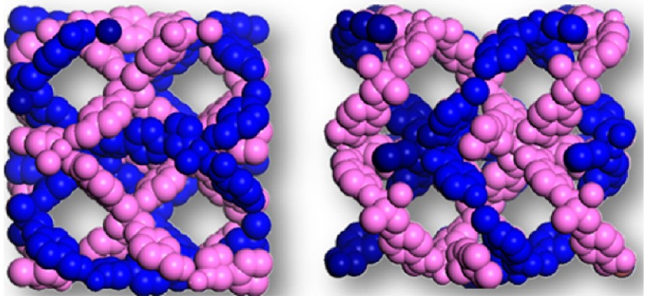

Figure 3. The space-filling view of **1** along the [100] and [010] directions.

solvent accessible void volume ratio in **1** is 47.8%. To further understand the structure of **1**, a topological analysis of the framework has been carried out using TOPOS. Two essential factors for investigating the topology of MOFs are the feature of coordination modes of metal ion/clusters and ligands in the structures. In compound **1**, the semirigid L ligands are in tetrahedral coordination geometry, which can be considered as a 4-connected node to connect four Co_2 clusters. Every dimetallic Co_2 building unit is connected to four L and two linear ligands, acting as a six-connected node. The linear bidentate ligands dib are transformed into edge during simplification. Thus, the framework of **1** features a 2-fold *sqc*422 net with point symbol of $\{4^2.5^4\}\{4^2.5^{10}.7^2.8\}$ (Figure S5 in the Supporting Information).

Structure of 2. Compound **2** crystallizes in triclinic space group $P\bar{1}$. As shown in Figure 4, there are two crystallographically independent Co atoms, one L ligand, and three dib sites in the asymmetric unit of **2**. Co(1) is in tetrahedral

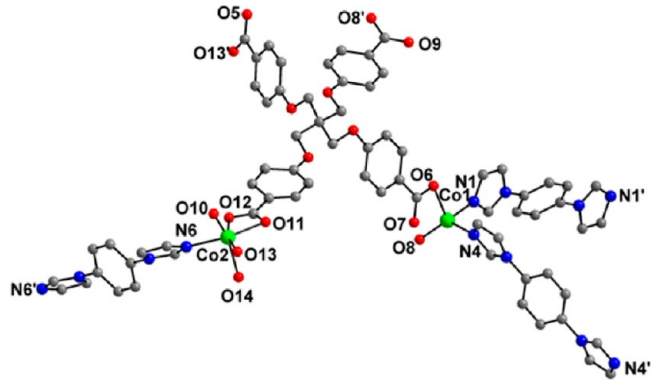

Figure 4. Coordination environments in **2**. Hydrogen atoms are omitted for clarity.

coordination surrounded by two N atoms from two dib and two μ-O atoms from two carboxylate groups. Co(2) is six-coordinated by three μ-O atoms from two carboxylate groups, one N atom of dib, and two terminal aqua molecules to form a distorted octahedron. The CoO_2N_2 tetrahedra and CoO_5N octahedra are linked together by L groups to produce a 2-dimensional (2-D) sheets extending along the $(\bar{1}01)$ direction, which are pillared by dib via sharing N atoms to form the 3-D framework (Figure 5). The single net of **2** contains multi-

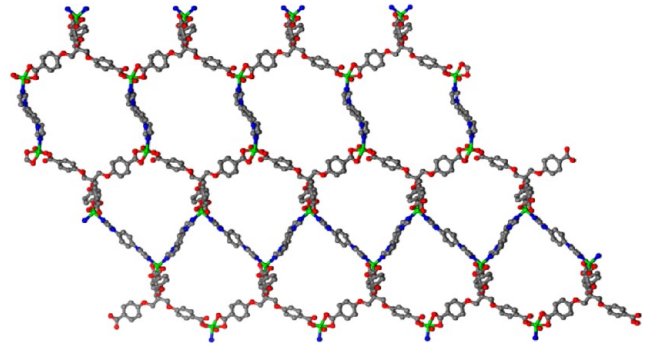

Figure 5. The independent single net in the interpenetrating framework of **2** (cobalt, green; carbon, gray; nitrogen, blue; oxygen, red). Hydrogen atoms are omitted for clarity.

dimensional channels, of which the biggest one is around 22.2 × 29.4 Å in the aperture. Due to the large void volume in the single net in **2**, quintuple equivalent networks interpenetrate each other to keep their stabilities of the whole structure (Figure 6). PLATON analysis gives the free void volume ratio

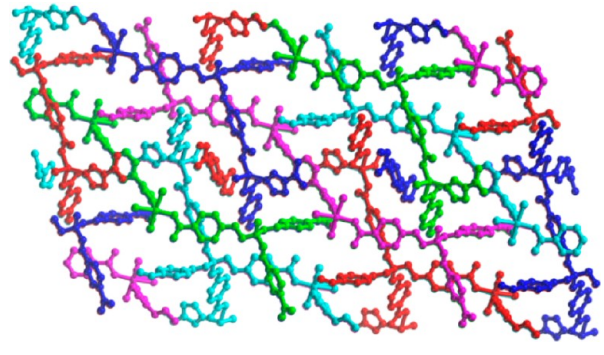

Figure 6. The space-filling view of **2** along the [100] direction.

dx.doi.org/10.1021/cg301094h | *Cryst. Growth Des.* 2012, 12, 5529−5534

of 18.7% in compound **2**. To simplify the network of **2**, Co(1) can be considered as a four-connected node, as it is connected by two L and two dib ligands. While Co(2) is linked by two L and one dib, and seen as three-connected nodes. They are linked by four-connected L and linear dib to form the network. Therefore, the whole framework of **2** can be simplified as a 3,4,4-connected net with point symbol of $\{6^3\}\{6^5.8\}\{6^6\}$, which is new topology with 5-fold interpenetration (Figure 7).

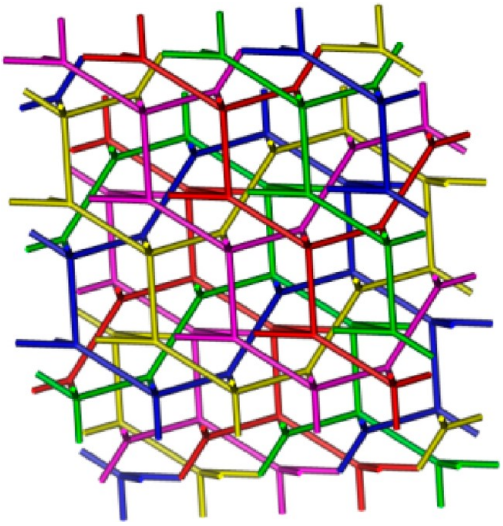

Figure 7. The simplified 5-fold interpenetrating networks of **2**.

Structure of 3. Compound **3** is a 3-D framework structure and crystallizes in the monoclinic space group *C*2/*c*. Similar to compound **1**, the structure features a dimetallic Co_2 cluster as its secondary building unit. Such dimetallic Co_2 clusters are connected by L to produce the 3-D framework, and the dibp are further coordinated to the skeleton by sharing N atoms with CoO_4N square pyramids. Such connection between the Co_2 clusters and the organic ligands creates 3-D intersected channels along the [100] (6.35 × 6.35 Å), [001] (4.25 × 3.50 Å), and [110] directions (8.60 × 3.21 Å) (Figure 8). Based on the PLATON analysis, the pore volume ratio is calculated to be 48.2%. TOPOS analysis reveals that the framework of **3** is a new 4,6-connected net with point symbol of $\{4^2.6^2.7^2\}$-$\{4^2.6^8.7^4.8\}$ (Figure S6 in the Supporting Information).

Structure of 4. The structure of **4** crystallizes in the tetragonal space group $I\bar{4}2d$. The asymmetric unit contains half of one Co atom, a quarter of L, and half dibp. The Co atom, which is located on the 2-fold axis, is octahedrally coordinated by four μ-O atoms from two carboxylate groups and two N atoms from two dibp (Figure 9). The linkage between Co atoms and dibp results in left-handed and right-handed helical tubes as shown in Figure 10. Such tubes are further connected by L to form the 3-D framework. In compound **4**, the Co atom is coordinated by two L and two dibp ligands; as a result, the Co atom can been seen as a four-connected node. Combined with the four-connected L nodes, the whole framework of **4** can be simplified as a 4,4-connected network with a point symbol, $\{8^6\}$, and extended point symbols, $\{8_6.8_6.8_6.8_6.8_6.8_6\}$-$\{8_4.8_6.8_7.8_7.8_7.8_7\}$ (Figure S7 in the Supporting Information).

It is interesting that the networks of both **1** and **2** are interpenetrated, which are constructed with the help of the second ligand dib, while for longer ligand dibp, no interpenetrating is occurring in compounds **3** and **4**. On the other hand, **1** and **3**, synthesized using DMF as the solvent, comprise Co_2 as their inorganic building unit. When a mixture of DMF and H_2O was used, a single Co unit acted as the connected nodes.

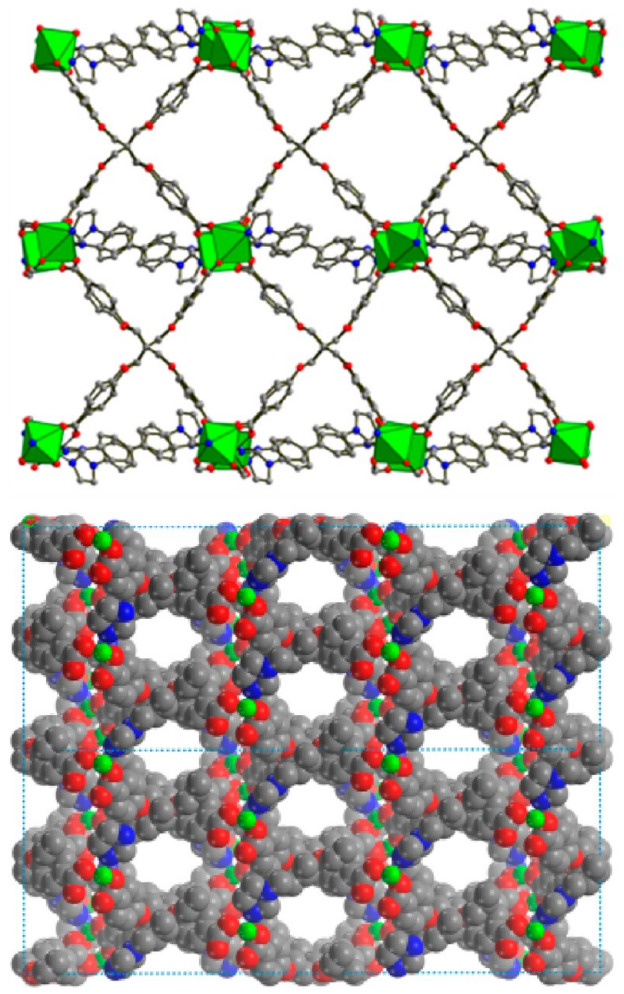

Figure 8. The structure of **3** viewed along the [100] direction (up) and the space-filling view along the [001] direction (down).

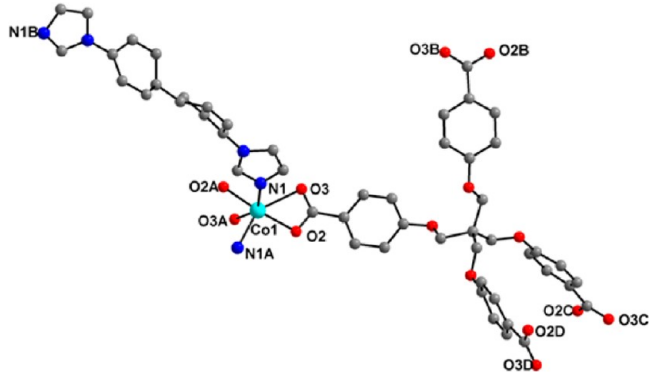

Figure 9. Coordination environments in **4** (cobalt, green; carbon, gray; nitrogen, blue; oxygen, red). Hydrogen atoms are omitted for clarity.

Thermal Stability. Thermogravimetric analysis (TGA) studies were conducted to characterize the thermal stability of **1**–**4**, which further confirms the extraframework DMF and water molecules (Figure 11). The TGA of **1** shows a continued

dx.doi.org/10.1021/cg301094h | *Cryst. Growth Des.* 2012, 12, 5529–5534

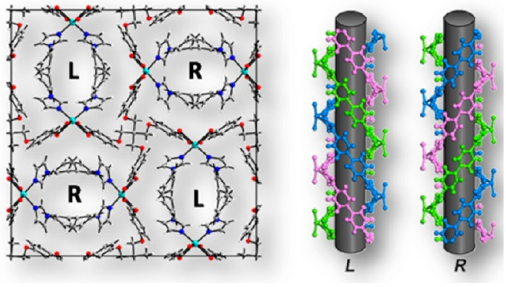

Figure 10. The structure of **4** viewd along the [001] direction showing the left-handed and right-handed helical tubes.

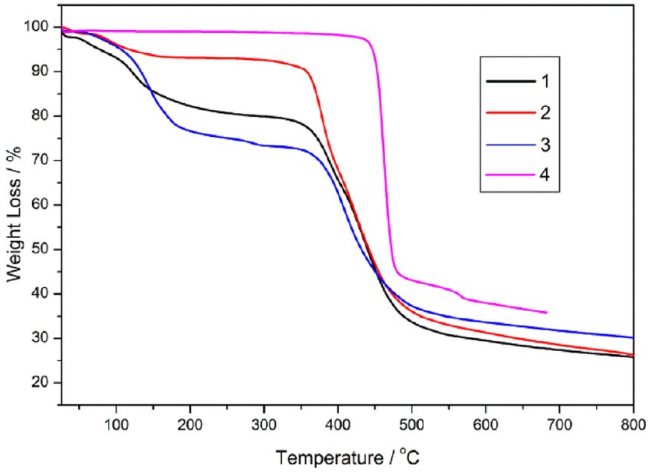

Figure 11. Thermogravimetric analyses data for **1**–**4**.

weight loss of about 20.8% from room temperature (RT) to 350 °C, implying the removal of DMF solvent molecules (calcd 18.9%), and then the compound starts degrading. Compound **2** shows a weight loss of 6.9% starting at RT and finishing at 180 °C, indicating the removal of water molecules (calcd 6.4%). No further weight loss was observed until 360 °C, at which the compound starts to decompose quickly. For **3**, the TGA curve displays a gradual weight loss of 26.7% between RT and 330 °C, corresponding to the release of 5 equiv of DMF per formula unit. After that it starts to decompose. Different from **1**–**3**, compound **4** exhibits no weight loss until 430 °C, at which it starts degrading rapidly. Based on these results, it is demonstrated that **1** and **3** containing channels show continued weight loss during heating until the frameworks decompose, while 5-fold interpenetrating framework of **2** and dense structure of **4** can be stable to 360 and 430 °C, respectively. Gas adsorption experiments on activated phase of compounds **1**–**3** (120 °C, 10^{-3} Torr) reveal negligible amounts of nitrogen, though they possess potential solvent accessible void volume.

Magnetic Properties. Since the Co(II) ions in **2** and **4** are linked though dib and dibp with the nearest distance of 6.936 Å and 8.479 Å, respectively, the magnetic interaction could be very weak. As a result, we only investigated the variable-temperature magnetic susceptibilities of **1** and **3**, which were measured on the field of 1000 Oe in the temperature range of 2.0–300 K (Figure 12). The $\chi_m T$ values at room temperature are 2.41 and 2.64 $cm^3\ mol^{-1}$ K, respectively, which are higher than the spin-only value for isolated Co(II) ion (1.86 cm^3 K mol^{-1}, $S = 3/2$), indicating an orbital contribution to the g-value.[14] Upon cooling, the $\chi_m T$ curves gradually decrease from room temperature and reach a minimum at 2.0 K (0.57 cm^3 K

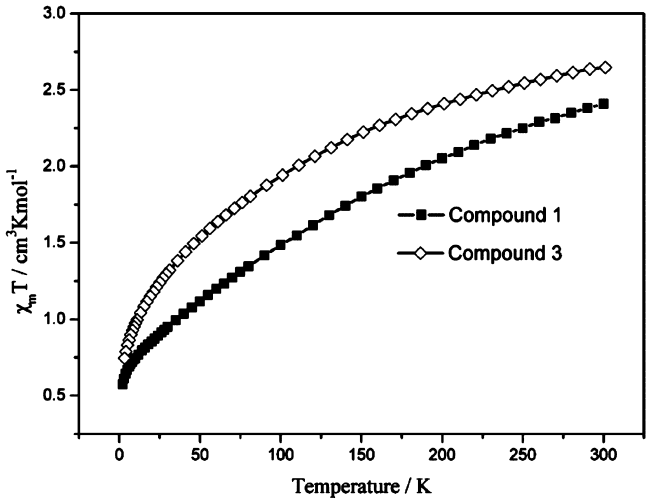

Figure 12. Temperature dependence of the $\chi_m T$ measured with a field of 1000 Oe in the range of 2–300 K for **1** and **3**.

mol^{-1} for **1**, 0.73 cm^3 K mol^{-1} for **3**). This behavior suggests the occurrence of antiferromagnetic interactions between adjacent Co(II) ions. The magnetic susceptibilities data follow the Curie–Weiss law ($\chi_m = C/(T - \theta)$) above 50 K with the C = 3.40 $cm^3\ mol^{-1}$ K and $\theta = -128.1$ K for **1**, and C = 3.11 cm^3 mol^{-1} K and $\theta = -57.7$ K for **3**. Deducing from the fitted Curie constant, the g value is about 2.69 and 2.57 for **1** and **3**, respectively. The negative Weiss constants also indicate antiferromagnetic interactions in **1** and **3**. Taking into account the coordinated environment of Co atoms in **1** and **3**, all of the Co ions are pentacoordinated in the square-pyramidal geometry. It is noted that an increase of the out-of-plane displacement of the Co ion from 0 (low-spin complex) to 0.74 Å (high-spin complex [Co(S-dept)$(NCS)_2$]) has been observered.[14b,14c] Complexes **1** and **3** show out-of-plane displacement of the Co(II) ion of 0.22–0.29 Å, which will stabilize the high-spin ($S = 3/2$) state of Co ions. In the same way, the studies of Hitchman showed that an increasing distortion from a square-pyramidal geometry, i.e., the angle between the apical and the basal bonds varying from 90 to about 110°, could result in a rapid decrease in the quartet-state energy.[15] For **1** and **3**, the N–Co–O angles are found from 90.12 to 105.5°, which also indicates the Co ions representing high-spin state. Thus regarding the structural features of **1** and **3**, the magnetic exchange pathway is probably through the carboxylate group unit by Co–O–C–O–Co linkage. In **1**, the two high-spin Co ions are interconnected via four O–C–O bridges with the Co(1)···Co(2) distance of 2.729 Å, while for **3**, there are two different Co_2 dimers in which they also are linked by four O–C–O bridges like in **1** with the Co(1)···Co(2) distance of 2.786 Å and the Co(3)···Co(4) distance of 2.807 Å. This might lead to the antiferromagnetic interactions between the Co ions in **1** and **3**.

CONCLUSIONS

In summary, we have synthesized four new cobalt MOFs constructed from the assembly of a semirigid tetracarboxylic ligand (H_4L) with linear bidentate ligands (dib and dibp). These compounds features quite different structures: **1** contains 3-D intersecting channels, although it is a 2-fold interpenetration of *sqc*422 nets; **2** comprises 5 interpenetrated nets with point symbol of $\{6^3\}\{6^5.8\}\{6^6\}$; **3** is a 3,4,4-

dx.doi.org/10.1021/cg301094h | *Cryst. Growth Des.* 2012, 12, 5529–5534

connected network with 3-D intersecting channels; **4** is a 3-D framework with extended point symbols $\{8_6.8_6.8_6.8_6.8_6.8_6\}$-$\{8_4.8_6.8_7.8_7.8_7.8_7\}$, which features helical tubes in its structure. The magnetic studies performed on **1** and **3**, which comprise dimetallic Co_2 as the building unit, show antiferromagnetic interactions in them.

■ ASSOCIATED CONTENT

Supporting Information

Powder X-ray diffraction patterns of **1**−**4**, simplified net of **1**, **3**, and **4**, and X-ray crystallographic files in cif format for **1**−**4**. This material is available free of charge via the Internet at http://pubs.acs.org.

■ AUTHOR INFORMATION

Corresponding Author

*E-mail: szm@ciac.jl.cn.

Notes

The authors declare no competing financial interest.

■ ACKNOWLEDGMENTS

Financial support for this research was provided by NSFC (21171162), SRF for ROCS (State Education Ministry) and CIAC startup fund. F.-Y.Y. thanks China Postdoctoral Science Foundation (No. 20110491329) for support.

■ REFERENCES

(1) (a) Xiao, B.; Peter J. Byrne, P. J.; Wheatley, P. S.; Wragg, D. S.; Zhao, X. B.; Fletcher, A. J.; Thomas, K. M.; Peters, L.; Evans, J. S. O.; Warren, J. E.; Zhou, W. Z.; Morris, R. E. *Nat. Chem.* **2009**, *1*, 289−294. (b) Yuan, D. Q.; Zhao, D.; Sun, D. F.; Zhou, H. C. *Angew. Chem., Int. Ed.* **2010**, *49*, 5357−5361. (c) Yan, Y.; Blake, A. J.; Lewis, W.; Barnett, S. A.; Dailly, A.; Champness, N. R.; Schröder, M. *Chem.—Eur. J.* **2011**, *17*, 11162−11170. (d) Ryan, P.; Broadbelt, L. J.; Sunrr, R. Q. *Chem. Commun.* **2008**, 4132−4134. (e) Kanoo, P.; Matsuda, R.; Higuchi, M.; Kitagawa, S.; Maji, T. K. *Chem. Mater.* **2009**, *21*, 5860−5866. (f) Kanoo, P.; Maji, T. K. *Eur. J. Inorg. Chem.* **2010**, *24*, 3762−3769.

(2) (a) Meek, S. T.; Greathouse, J. A.; Allendorf, M. D. *Adv. Mater.* **2011**, *23*, 249−267 and references therein. (b) Horcajada, P.; Serre, C.; Vallet-Regí, M.; Sebban, M.; Taulelle, F.; Férey, G. *Angew. Chem., Int. Ed.* **2006**, *45*, 5974−5978.

(3) (a) Chen, B. L.; Xiang, S. C.; Qian, G. D. *Acc. Chem. Res.* **2010**, *43*, 1115−1124. (b) Guo, Z. Y.; Xu, H.; Su, S. Q.; Cai, J. F.; Dang, S.; Xiang, S. C.; Qian, G. D.; Zhang, H. J.; O'Keeffe, M.; Chen, B. L. *Chem. Commun.* **2011**, *47*, 5551−5553. (c) Chen, B. L.; Wang, L. B.; Xiao, Y. Q.; Fronczek, F. R.; Xue, M.; Cui, Y. J.; Qian, G. D. *Angew. Chem., Int. Ed.* **2009**, *48*, 500−503. (d) Chen, B. L.; Wang, L. B.; Zapata, F.; Qian, G. D.; Lobkovsky, E. B. *J. Am. Chem. Soc.* **2008**, *130*, 6718−6719. (e) Jiang, H.-L.; Tatsu, Y.; Lu, Z.-H.; Xu, Q. *J. Am. Chem. Soc.* **2010**, *132*, 5586−5587.

(4) (a) Corma, A.; García, H.; Xamena, F. X. L. *Chem. Rev.* **2010**, *110*, 4606−4655. (b) Jiang, H.-L.; Liu, B.; Akita, T.; Haruta, M.; Sakurai, H.; Xu, Q. *J. Am. Chem. Soc.* **2009**, *131*, 11302−11303. (c) Jiang, H.-L.; Xu, Q. *Chem. Commun.* **2011**, *47*, 3351.

(5) (a) Farha, O. K.; Yazaydın, A. Ö.; Eryazici, I.; Malliakas, C. D.; Hauser, B. G.; Kanatzidis, M. G.; Nguyen, S. T.; Snurr, R. Q.; Hupp, J. T. *Nat. Chem.* **2010**, *2*, 944−948. (b) Lan, Y. Q.; Jiang, H. L.; Li, S. L.; Xu, Q. *Adv. Mater.* **2011**, *23*, 5015−5020. (c) Zheng, S. T.; Bu, J. J.; Wu, T.; Chou, C.; Feng, P. Y.; Bu, X. H. *Angew. Chem., Int. Ed.* **2011**, *50*, 8858−8862.

(6) (a) Liang, L. L.; Zhang, J.; Ren, S. B.; Ge, G. W.; Li, Y. Z.; Du, H. B.; You, X. Z. *CrystEngComm* **2010**, *12*, 2008−2010. (b) Liang, L. L.; Ren, S. B.; Wang, J.; Zhang, J.; Li, Y. Z.; Du, H. B.; You, X. Z. *CrystEngComm* **2010**, *12*, 2669−2671. (c) Liang, L. L.; Ren, S. B.; Zhang, J.; Li, Y. Z.; Du, H. B.; You, X. Z. *Dalton Trans.* **2010**, *39*, 7723−7726. (d) Tian, J.; Motkuri, R. K.; Thallapally, P. K.; McGrail, B. P. *Cryst. Growth Des.* **2010**, *10*, 5327−5333. (e) Liu, T. F.; Lu, J.; Lin, X.; Cao, R. *Chem. Commun.* **2010**, *46*, 8439−8441. (f) Liu, T. F.; Lü, J.; Guo, Z. G.; Proserpio, D. M.; Cao, R. *Cryst. Growth Des.* **2010**, *10*, 1489−1491. (g) Liu, T. F.; Lü, J.; Tian, C. B.; Cao, M. N.; Lin, Z. J.; Cao, R. *Inorg. Chem.* **2011**, *50*, 2264−2271. (h) Guo, Z. G.; Cao, R.; Wang, X.; Li, H. F.; Yuan, W. B.; Wang, G. J.; Wu, H. H.; Li, J. *J. Am. Chem. Soc.* **2009**, *131*, 6894−6895. (i) Kim, T. K.; Suh, M. P. *Chem. Commun.* **2011**, *47*, 4258−4260. (j) Kim, H.; Suh, M. P. *Inorg. Chem.* **2005**, *44*, 810−812. (k) Kishan, M. R.; Tian, J.; Thallapally, P. K.; Fernandez, C. A.; Dalgarno, S. J.; Warren, J. E.; McGrail, B. P.; Atwood, J. L. *Chem. Commun.* **2010**, *46*, 538−540. (l) Thallapally, P. K.; Tian, J.; Kishan, M. R.; Fernandez, C. A.; Dalgarno, S. J.; McGrail, P. B.; Warren, J. E.; Atwood, J. L. *J. Am. Chem. Soc.* **2008**, *130*, 16842−16843.

(7) (a) Zhang, J.; Chew, E.; Chen, S.; Pham, J. T. H.; Bu, X. *Inorg. Chem.* **2008**, *47*, 3495−3497. (b) Clegg, J. K.; Iremonger, S. S.; Hayter, M. J.; Southon, P. D.; Macquart, R. B.; Duriska, M. B.; Jensen, P.; Turner, P.; Jolliffe, K. A.; Kepert, C. J.; Meehan, G. V.; Lindoy, L. F. *Angew. Chem., Int. Ed.* **2010**, *49*, 1075−1078. (c) Zheng, S. T.; Zuo, F.; Wu, T.; Irfanoglu, B.; Chou, C.; Nieto, R. A.; Feng, P. Y.; Bu, X. H. *Angew. Chem., Int. Ed.* **2011**, *50*, 1849−1852.

(8) (a) Ren, S. B.; Zhou, L.; Zhang, J.; Zhu, Y. L.; Li, Y. Z.; Du, H. B.; You, X. Z. *CrystEngComm* **2010**, *12*, 1635−1638. (b) Liang, L. L.; Ren, S. B.; Zhang, J.; Li, Y. Z.; Du, H. B.; You, X. Z. *Cryst. Growth Des.* **2010**, *10*, 1307−1311.

(9) Guo, M.; Sun, Z. M. *J. Mater. Chem.* **2012**, *22*, 15939−15946.

(10) Laliberté, D.; Maris, T.; Wuest, J. D. *J. Org. Chem.* **2004**, *69*, 1776−1787.

(11) *SMART* and *SAINT* (software packages); Siemens Analytical X-ray Instruments, Inc.: Madison, WI, 1996.

(12) *SHELXTL Program*, version 5.1; Siemens Industrial Automation, Inc.: Madison, WI: 1997.

(13) Spek, A. L. *PLATON99, A Multipurpose Crystallographic Tool*; Utrecht University, Utrecht: The Netherlands, 1999.

(14) (a) Kahn, O. *Molecular Magnetism*; VCH: Weinheim, Germany, 1993. (b) Kapoor, R.; Kataria, A.; Venugopalan, P.; Kapoor, P.; Jundal, G.; Corbella, M. *Eur. J. Inorg. Chem.* **2005**, 3884−3893. (c) Jia, Z. Q.; Sun, X. J.; Hu, L. L.; Tao, J.; Huang, R. B.; Zheng, L. S. *Dalton Trans.* **2009**, 6364−6367.

(15) (a) Jean, Y. *Molecular Orbitals of Transition Metal Complexes*; Oxford University Press: 2005; p 60. (b) Hitchman, M. A. *Inorg. Chim. Acta* **1978**, *248*, 237−245.